

Study of the $\text{Mg}^{26}(p, p'\gamma)$ Reaction Mechanism at Low Energies

H. HULUBEI, N. MARTALOGU, M. IVAȘCU, N. SCÎNTEI, A. BERINDE, I. NEAMU, AND J. FRANZC

Institute for Atomic Physics, Bucharest, Rumania

(Received 7 April 1965)

The angular distribution and $p'\text{-}\gamma$ angular correlations of the protons inelastically scattered on the first two 2^+ excited states of Mg^{26} were measured at several energies of the incident protons between 5.67 and 6.46 MeV. The angular correlation of the inelastically scattered protons on the Mg^{26} second excited state is of the type $0^+ \rightarrow J^\pi \rightarrow 2^+ \gg 2^+ \rightarrow 0^+$, where the heavy arrow indicates the unobserved cascade γ rays. The angular distributions and correlations corresponding to the second level of Mg^{26} ($Q = -2.94$ MeV) are in good agreement with the predictions of the statistical model. In the case of the protons which populate the first level ($Q = -1.81$ MeV) the angular distribution varies strongly with the energy, indicating a violation of the hypotheses on which the statistical model is based. The angular correlations corresponding to the excitation of this level likewise agree only in some cases with the predictions of the statistical model. The difference in behavior of the angular distribution and angular correlations on the two levels is attributed to the differences in value of the transmission coefficients $T_l(E)$. Angular correlations for $\text{Mg}^{26}(p, p'\gamma)$, $Q = -1.81$ MeV at energies higher than 6 MeV also suggest some contribution of the direct-interaction mechanism.

THE aim of the present work is to study the $\text{Mg}^{26}(p, p')$ reaction mechanism for some energies at about 6 MeV, through measurements of the excitation functions, angular distribution, and angular correlations corresponding to the excitation of the first two energy levels of the target. There is, so far, little information regarding the mechanism of the inelastic scattering of protons on Mg^{26} . The angular-distribution measurements at 18.1-MeV energy of the incident protons reported by Schrank, Warburton, and Daehnick¹ show forward peaks that are characteristic of direct interaction. An important direct-interaction (D.I.)-mechanism contribution of about 60% in the case of inelastic scattering on the Mg^{26} second excited state within the 8.3–10.5-MeV energy range was evidenced by Häusser, Von Brentano, and Mayer Kuckuk² in the analysis of the differential-cross-section statistical fluctuations. At low energies some indications about the reaction mechanism can be obtained from the measurements made by Miura *et al.*³ on the γ -radiation yield resulting from the inelastic scattering of protons with energies up to 5.7 MeV that leaves the Mg^{26} on one of its two first excited levels. The yield of the 1.81-MeV γ radiation corresponding to the transitions from the first level to the ground state, and of the 1.13-MeV γ radiation resulting from the transition between the second and the first levels, shows a resonant structure.

This points to the preponderance of the compound-nucleus (C.N.) mechanism at energies of the incident protons lower than 5.7 MeV.

On the other hand, in the case of the other even-even isotope Mg^{24} , measurements of angular distribution and angular correlations made at energies of about 6 MeV^{4,5}

did not allow an exact specification of the reaction mechanism involved. In fact, the theoretical analysis undertaken by Sheldon⁶ could not make the experimental results agree either with the correlations computed on the basis of the statistical model or with those computed on the basis of the distorted-wave direct-interaction theory. It is possible, in the cases analyzed, for both reaction mechanisms to be in competition, with a predominance of the C.N. mechanism having an excitation of too few levels in the compound nucleus for the statistical theory to be applicable. A great weighting for the C.N. mechanism is to be expected, since at low energies of the bombarding protons practically only the first Mg^{24} level is excited. In the case of Mg^{26} , however, and under the same energy conditions, the bombarding protons excite the first two levels with comparable cross sections, so that the compound nucleus can decay through an increased number of channels. This might lead, through competition, to a decrease of the C.N. contribution to a given reaction channel. Under these circumstances the D.I. mechanism might be easier to put in evidence. As a means for studying the $\text{Mg}^{26}(p, p')$ reaction mechanism, the measurements of angular distribution and angular correlation between the inelastically scattered protons and the de-excitation γ rays were used in this work.

The scattering differential cross section can be expressed in the general form

$$\sigma(\theta) = \sum_K A_K P_K(\cos\theta), \quad (1)$$

where $P_K(\cos\theta)$ are Legendre polynomials of order K , and A_K are coefficients depending on the mechanism involved in the reaction.

If the inelastic-scattering reaction takes place through excitation of an isolated resonance in the compound nucleus, then only the coefficients with even K do not vanish, a symmetric angular distribution around $\theta = 90^\circ$ being obtained. The maximum value of K is related to

¹ G. Schrank, E. K. Warburton, and W. W. Daehnick, *Phys. Rev.* **127**, 2159 (1962).

² O. Häusser, P. Von Brentano, and T. Mayer Kuckuk, *Phys. Letters* **12**, 226 (1964).

³ I. Miura, T. Wakatsuki, Y. Hirao, and E. Okada, *J. Phys. Soc. Japan* **14**, 239 (1959).

⁴ F. Seward, *Phys. Rev.* **114**, 514 (1959).

⁵ H. A. Lackner, G. F. Dell, and H. J. Hausman, *Phys. Rev.* **114**, 560 (1959).

⁶ E. Sheldon, *Rev. Mod. Phys.* **35**, 795 (1963).

the maximum value of the orbital angular momentum l by the relation $K_{\max} \geq 2l_{\max}$. Each coefficient A_K varies strongly with the energy around the isolated resonance, the angular distribution maintaining its shape. When in the compound nucleus only a restricted number of resonance levels with different parities are excited, because of the interference between partial waves with opposite parities, coefficients A_K with odd K appear in the angular-distribution formula. The presence of these terms leads to asymmetric angular distributions around $\theta=90^\circ$ that indicate strong changes both in absolute value and in shape for comparatively small energy changes. Finally, if a great level density characterizes the compound nucleus, so that the hypotheses of the statistical theory are applicable, the interference terms related to the coefficients A_K with odd K vanish and the angular distribution again becomes symmetric at about 90° . The high value of the coefficient A_0 as compared to the other coefficients and a monotonic variation of $\sigma(\theta)$ with the energy are characteristic of these distributions.

The direct-interaction mechanism generally predicts asymmetric angular distributions at about 90° , i.e., the presence of some odd- K A_K coefficients in relation (1). But, in contrast with the case of the C.N. mechanism with excitation of a restricted number of resonances, the D.I. angular distribution varies weakly with the energy of the incident protons. For instance, the plane-wave direct-interaction theory predicts a differential cross section of the form $j_l^2(qR)$. In this formula j_l is the spherical Bessel function of order l , R is the interaction radius, and $\mathbf{q} = \mathbf{k}_p - \mathbf{k}_{p'}$ is the momentum transfer, where \mathbf{k}_p and $\mathbf{k}_{p'}$ are, respectively, the momenta of the incident and emergent protons.

In the distorted-wave Born approximation (DWBA), which constitutes a more realistic description of the D.I. process, these characteristics, i.e., a strong variation with θ and a weak variation with energy of the differential cross section, remain unaltered.

The angular correlation between the inelastically scattered protons and the de-excitation γ rays of the residual nucleus is another means of studying the reaction mechanism. In our work the angular correlations between the protons inelastically scattered on the first two Mg^{26} excited states ($Q = -1.81$ MeV and $Q = -2.94$ MeV, both having a 2^+ spin and parity) and the γ rays corresponding to the transition from the first level to the ground state 0^+ were simultaneously measured. In the case of the angular correlations of protons exciting Mg^{26} to its second state, the $2^+ \rightarrow 2^+$ cascade γ radiations were not detected. The angular-correlation function corresponding to the first excited level, which is of the type $0^+ \rightarrow J^\pi \rightarrow 2^+ \rightarrow 0^+$, is of the general form⁷

$$W(\theta_p, \theta_\gamma, \pi) = a + b \sin^2(\theta_\gamma - \theta_0) + c \sin^2(\theta_\gamma - \theta_0') \quad (2)$$

where π is the azimuthal angle corresponding to the

situation where the proton and the γ -radiation detectors are in the same plane as the incident beam, on either side of the latter. Although the general form (2) of the angular-correlation function is not dependent on the reaction mechanism, valuable knowledge can, however, be derived from the values of the quantities a , b , c , θ_0 , and θ_0' .

Thus, in the case of a C.N. mechanism in which an isolated resonance or—for the applicability of the statistical hypothesis and of the continuum—a sufficiently high number of levels is excited, the condition $c > b$ is fulfilled. Besides, the statistical model requires that $a \gg c$. In this case an important symmetry feature of the angular-correlation function is

$$W(\theta_{p'}, \theta_\gamma, \pi) = W(\pi - \theta_{p'}, \pi - \theta_\gamma, \pi). \quad (3)$$

These properties of the angular-correlation function may no longer be satisfied when in the compound nucleus a limited number of levels is excited and the hypotheses of the statistical theory are violated. In this case we can expect striking variations of the angular-correlation function with energy, owing to interference effects.

In direct reactions the angular-correlation function depends on the approximations made in describing the process. Thus, when the wave functions describing the ingoing and outgoing protons are approximated by plane waves and the dependence on spin of the interaction forces is neglected, one obtains⁸ $a = c = 0$ and $\theta_0 = \theta_R$, where θ_R is the classical recoil angle of the nucleus.

Maintaining the plane-wave approximation but taking into account the spin-flip amplitude, Banerjee and Levinson⁹ have obtained $b > a > c$ and $\theta_0 = \theta_0' = \theta_R$. In the DWBA theory, neglecting the spin-flip amplitude, Banerjee and Levinson obtain $c = 0$, $b > a$; and in the case of C^{12} , numerical computations show that the angle θ_0 is near θ_R and shifts in the same sense. The same form for the angular-correlation function was obtained by Blair and Wilets¹⁰ in the adiabatic approximation, with the difference that $\theta_0 = \frac{1}{2}\pi - \frac{1}{2}\theta_p$, where θ_p is the angle of the protons elastically scattered in the direction of the detector. Taking into account the spin-flip contribution in the DWBA theory leads to the appearance of the supplementary terms $c \sin^2(\theta_\gamma - \theta_0')$. Generally $c < b$. If this relation were not valid, the D.I. angular correlations could hardly be distinguishable from the C.N. correlations.

The direct interaction requires a weak variation of the angular-correlation-function parameters with energy.

As regards the dependence of the parameter θ_0 on the recoil angle θ_R , the fact should be mentioned that, while the numerical computation made by Banerjee and Levinson in the case of C^{12} shows that θ_0 is close to θ_R ,

⁸ G. R. Satchler, Proc. Phys. Soc. **A68**, 1037 (1955).

⁹ M. K. Banerjee and C. A. Levinson, Ann. Phys. (N. Y.) **2**, 449 (1957).

¹⁰ J. S. Blair and L. Wilets, Phys. Rev. **121**, 1493 (1961).

⁷ I. Sawicki, Nucl. Phys. **7**, 503 (1958).

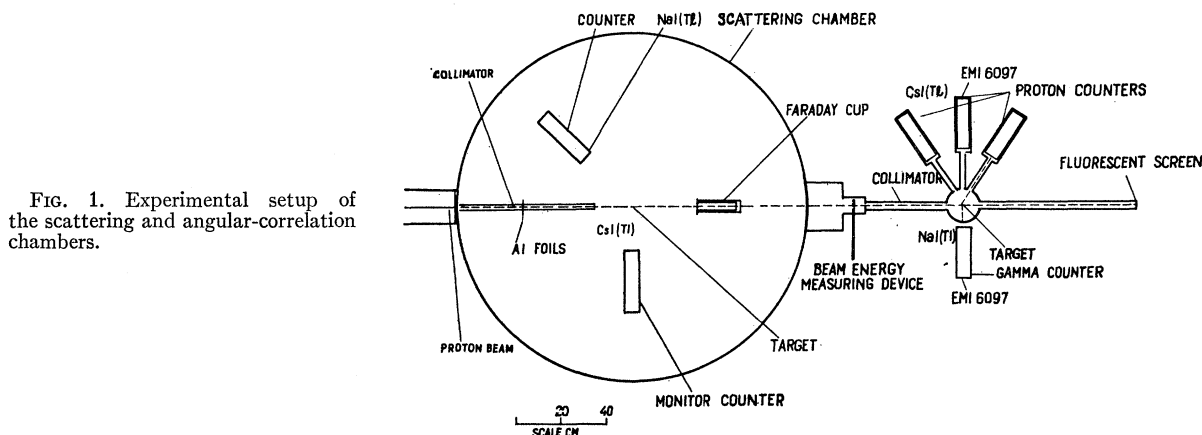


FIG. 1. Experimental setup of the scattering and angular-correlation chambers.

Sheldon's calculation for the case of Mg²⁴ and other elements does not indicate any relation between these two angles.

For the angular correlation of type $0^+ \rightarrow J^\pi \rightarrow 2^+ \rightarrow 2^+ \rightarrow 0^+$, where the heavy arrow indicates the unobserved cascade radiation, no calculations based on direct interaction have so far been published. Computation formulas based on the statistical model were elaborated by Sheldon¹¹ for this type of angular correlation.

In our work, as a basis for comparison with the angular-distribution and angular-correlation experimental data, the statistical model, for which there exist concrete computation formulas, was taken into consideration. In the case of the experimental angular distribution and angular correlations corresponding to the first level, curves of the form (1) and (2) were drawn; the deviations from the curves computed by means of the statistical model were interpreted in terms of the values of the parameters A_K , a , b , c , θ_0 and θ_0' .

EXPERIMENTAL METHOD

The proton source was the cyclotron of the Institute for Atomic Physics in Bucharest. The energy of the protons was obtained by determining the excitation function of the Mg²⁴(*p, p'*)Mg²⁴ ($Q=1.37$ MeV) reaction at $\theta_p=90^\circ$, whose resonances were compared with the published data.^{3,4} Energy measurements using the total proton absorption in Al foils were also made. The energy spread of the proton beam at the center of the target was about 1%. The geometry of the system for the measurement of angular distribution and angular correlations is shown in Fig. 1. It consists of a 150-cm diam. scattering chamber and a 13-cm-diam. correlation chamber. The scattering chamber is equipped with four mobile arms. On two of these arms two scintillation counters were mounted; one of them, consisting of a 1-mm-thick NaI(Tl) crystal and a AVP 53 photomultiplier, was employed for angular-distribution measure-

ments, and the other, composed of a 0.8 mm-thick CsI(Tl) crystal and a RCA 6655 photomultiplier, was placed at 90° and used as a monitor. On the remaining two arms were fixed the collimation system of the incident beam and the Faraday cup for the measurement of the absolute cross section. The collimator, made of two tantalum tubes with slits in disks made of the same material, reduced the beam incident on the target situated in the center of the chamber to a 3-mm-diam. circular cross section. Between the two collimating tubes was a disk with ten holes, nine of which were covered with aluminum foils of different thicknesses necessary to measure the excitation functions through the variation of the incident proton energy. A slit disk at a potential of 1000 V was put in front of the Faraday cup to prevent the escape of the secondary electrons.

By rotating the arms, the collimator and the Faraday cup could be removed from the direction of the incident beam, thus letting the beam enter the correlation chamber. After passing through the target situated in the center of the correlation chamber, the beam was made visible on a fluorescent screen at the end of a brass tube. Before entering the correlation chamber the beam was collimated by means of 4-mm-diam. tantalum slits. The construction of the correlation chamber allowed the simultaneous measurement of three correlation curves corresponding to the angles $\theta_p'=60^\circ$, 90° , and 120° of the proton detectors and to the azimuth $\varphi=\pi$. The proton detectors employed in the correlation experiment were made up of 0.8-mm-thick CsI(Tl) crystals and EMI 6097 photomultipliers. As a γ -radiation detector, a 3.8-cm-diam., 2.5-cm-high NaI(Tl) crystal mounted on an EMI 6097 photomultiplier was used. The crystals of the proton counters were placed at a distance of 19 cm from the target and the γ -radiation counter at a distance of 8 cm. The crystals of the proton detectors, situated in vacuum, were linked to the outside photomultipliers by glass light guides. Between the angular-distribution chamber and the correlation chamber was mounted the device for energy measurement by the method of total absorption in Al foils.

¹¹ E. Sheldon, Phys. Rev. **133**, B732 (1964).

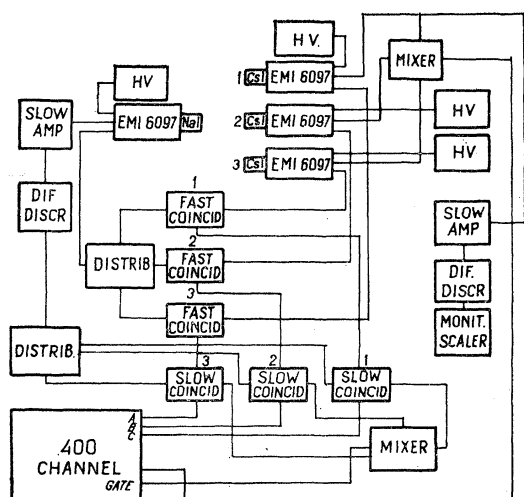


FIG. 2. Block diagram of the fast-slow coincidence circuit.

MgO enriched up to 96% in Mg^{26} was used as a target. The MgO target was 1 mg/cm² thick and had been obtained by the electrophoresis of a fine MgO powder suspension in acetone. The backing of the target was a 0.25 mg/cm²-thick gold foil.

In the angular-distribution measurements the proton spectra were recorded by means of a 400-channel pulse-height analyzer. The energy resolution of the first Mg^{26} inelastic peak was about 6%.

A block diagram of the electronic coincidence circuit is shown in Fig. 2. It includes three fast-slow coincidence systems connected to the amplitude multichannel analyzer. The fast-rising pulses of the proton counters were fed to a corresponding Rossi-type fast-coincidence circuit. The fast-rise pulse of the γ counter reached the other entrance of each of the fast-coincidence circuits through a distributor. The resolving time of the fast-coincidence circuits was 22 nsec. The pulses from the output of the fast-coincidence circuits were fed to three slow-coincidence circuits. The other entrance of each slow-coincidence circuit was fed by the slow-rise γ pulse obtained by passage through a wide-window differential discriminator and a distributor, after a previous amplification of the slow-rise signal given by the γ counter. The slow coincidences had two outputs, one of them connected to a mixer and the other to the controlling circuits (A, B, and C) of the 400-channel pulse-height analyzer. To each input A, B, or C correspond 100 of the channels of the multichannel analyzer, on which the spectrum of the protons detected by each of the three counters was displayed. The gate of the multichannel analyzer was fed by both the slow-rise pulses from the three proton counters, and the pulses proceeding from the slow coincidences, after both had been put through their respective mixers. It therefore resulted that a proton pulse was analyzed only if the control of the analysis gate had been opened, that is, if a fast coincidence (p , γ simultaneity) and a slow one (γ quantum of desired energy) had occurred.

The monitoring of the proton beam incident on the target was made by counting the protons elastically scattered at a 60° angle. In Fig. 3 a typical γ -ray spectrum is shown. The hatched part indicates the region of the spectrum used in the coincidence measurements. The random coincidences were evaluated by making a comparison of the gated proton spectrum and the ungated proton spectrum measured at the beginning and at the end of each run. Figure 4 shows an example of such spectra. The points represent the coincidence spectrum of the 1.81-MeV γ rays with the corresponding protons, and the solid curve the noncoincident proton spectrum. Both spectra correspond to the same number of incident protons. As the elastically scattered protons cannot give rise to actual coincidences, the elastic peak in the gated spectrum is attributed wholly to random coincidences. Since the inelastically scattered protons have the same chance to produce random coincidences, the number of these can be computed with the help of the two spectra. If N_e and N_i are the numbers of protons contained, respectively, in the elastic and the inelastic peaks of the noncoincident spectrum, and N_{ea} the number of events in the elastic peak of the coincident proton spectrum, then the number of random coincidences in the inelastic peak will be $N_{ia} = N_{ea}(N_i/N_e)$. In Fig. 4, the noncoincident proton spectrum, if read on the left-hand scale, represents the spectrum of the random coincidences. In our correlation measurements the ratio of the actual to random coincidences varied between 2:1 and 15:1.

RESULTS AND DISCUSSION

Excitation functions. In order to select the incident proton energies for the angular distribution and angular-correlation measurements, the excitation functions of the protons inelastically scattered on the first and on the second Mg^{26} excited states were measured at $\theta_{lab} = 90^\circ$.

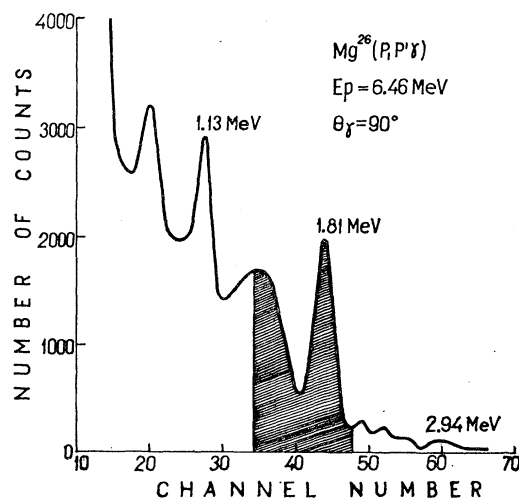


FIG. 3. Gamma-ray spectrum obtained through the bombardment of the Mg^{26} target with 6.46-MeV protons. The hatched area indicates the part of the gamma spectrum used in the coincidence measurements.

The results obtained for energies of the incident protons lying between 5.16 and 6.46 MeV are shown in Fig. 5. The excitation function corresponding to the first level ($Q = -1.81$ MeV) displays a maximum at the energy of 5.67 MeV, and the one corresponding to the second level, a maximum at 5.55 MeV. The maximum that appears in the excitation function for $Q = -2.94$ MeV seems to correspond to the resonance observed by Miura *et al.*² around the energy of 5.45 MeV. At the bombardment energies around 6 MeV used in this work, the Al²⁷ compound-nucleus excitation energy is about 14 MeV. Within this range of the excitation energy the level density of the Al²⁷ compound nucleus is comparatively high so that it is to be expected that the resonances in the excitation functions are caused by the excitation of quite a large group of levels. Since the form of the angular distribution of the proton leaving Mg²⁶ in its second excited state does not change with the energy, the resonance at 5.55 MeV must appear in the total cross section as well as in the yield of γ radiation. Besides, the shape of the angular distributions of the protons inelastically scattered on the first Mg²⁶ level varies strongly with the energy, so that the maximum observed in the excitation function from one angle only does not necessarily imply the existence of a resonance in the inelastic total cross section corresponding to that level. This fact is made evident by the excitation functions of the inelastic total cross sections obtained through integration of the angular distributions, shown in Fig. 6. In the excitation function of the inelastic

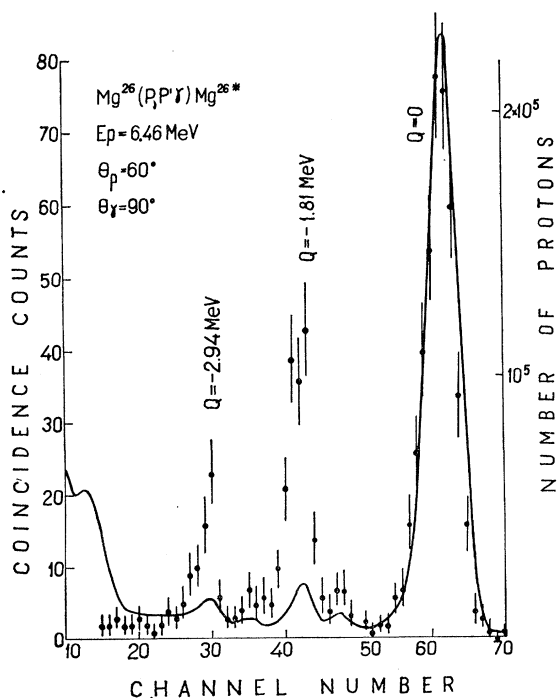


FIG. 4. Spectrum of the protons scattered on the Mg²⁶ target. The proton spectrum is shown in coincidence with the 1.81-MeV gamma rays by the points. The solid curve represents the non-coincident proton spectrum (right-hand scale) and at the same time the random-coincidence spectrum (left-hand scale).

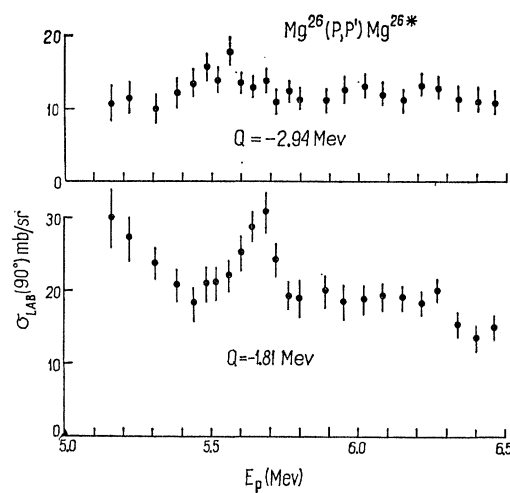


FIG. 5. The excitation functions of the inelastically scattered protons on the first two Mg²⁶ excitation levels, measured at 90° in the laboratory system.

integrated cross section corresponding to the first level, there is no visible increase of the cross section at $E_p = 5.67$ MeV. Both excitation functions show a maximum at the energy of 5.92 MeV. This maximum is probably caused by a fluctuation of the density and parameters of the compound-nucleus levels and not by the existence of an isolated resonance level. This conclusion is probably valid also in the case of other resonances arising in the Mg²⁶(p, p') reaction at energies near the domain investigated by us. The excitation functions of the total cross section are compared in Fig. 6 with the predictions of the statistical model expressed through the solid curves. The computations were made by using Sheldon's⁶ formulas in the $l \leq 2$ approximation. The transmission coefficients $T_l(E)$ that occur in the formulas were obtained through interpolation from the graphs published by Meldner and Lindner¹² and computed by means of the Perey optical potential for protons. Since the transmission coefficient T_1 has a resonance in the region of Mg²⁶ the value obtained through interpolation is subject to errors higher than those affecting the other two coefficients T_0 and T_2 used in the calculation. The computation formulas published by Sheldon were obtained in the approximation of two decay channels for the compound nucleus, namely, to the ground state and to the first excited state 2^+ . In our calculation the computation formulas were suitably modified to take into account three decay channels for the compound nucleus, namely, to the ground state 0^+ and to the first two excited states, both having spin and parity 2^+ . This three-channel approximation brings the theoretical cross sections near enough to the experimental ones in the case of the second Mg²⁶ excited state. In the case of inelastic scattering on the state $Q = -2.94$ MeV the agreement would be still better if exact values were employed for the transmission coefficient T_1 , the value of which, obtained through interpolation, had

¹² H. Meldner and A. Lindner, Z. Physik **180**, 362 (1964).

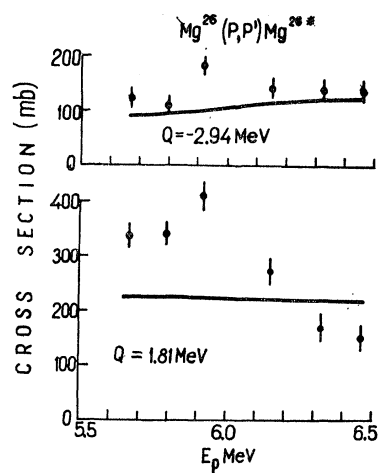


FIG. 6. The excitation functions of the total scattering cross sections on the first two Mg^{26} excitation levels, obtained by integrating the angular distributions.

been underestimated. The agreement between theory and experiment, in the case of the excitation function corresponding to the scattering on the first excited state, is poor.

Angular Distributions. In Fig. 7 are shown the angular distributions of the protons that leave Mg^{26} in the first excited state ($Q = -1.81$ MeV), measured at energies of 5.67, 5.80, 5.92, 6.15, 6.33, and 6.46 MeV. The error in the evaluation of the absolute cross section was estimated as 10%. The solid curves were calculated by means of the statistical model, and the dashed curves show distributions of type (1) fitted to the experimental data by using the least-squares method. The A_K coefficients thus obtained are listed in Table I. As may be seen in Fig. 7, the agreement with the predictions of the statistical model is poor. The strong variations of the angular distributions with energy suggests the preponderance of the compound-nucleus mechanism with a violation of the hypotheses on which the statistical model is based. These experimental data show that, although the excitation energy of the Al^{27} compound nucleus is high enough, the levels are not sufficiently dense to cancel, by averaging, the interference effects due to C.N. levels having opposite parities. The interference terms show up through the presence of the A_K coefficients with odd K in Table I. The coefficients A_1 and A_3 have maximum values around the energy of 5.92 MeV, where the total cross section has a maximum too.

It is also quite possible for the terms A_1 and A_3 to be

TABLE I. Experimental values of the parameters A_K of the angular distributions [Eq. (1)].

E_p (MeV)	A_0	A_1	A_2 (mb/sr)	A_3	A_4
5.67	23.93	-1.46	-9.31	-2.20	-4.54
5.80	27.24	-10.23	12.81	2.89	0.15
5.92	32.77	-12.10	25.54	9.12	-6.03
6.15	21.52	-5.62	5.44	-8.35	2.12
6.33	13.22	-0.71	-9.27	-3.96	-1.82
6.46	12.03	2.21	-5.31	-3.03	-0.71

partly due to a direct-interaction contribution, but the weight of this contribution cannot be established from the present experimental angular-distribution data.

The angular distributions of the protons that excited the second 2^+ of Mg^{26} level are drawn in Fig. 8 and compared with the predictions of the statistical model. These distributions are practically isotropic, in good agreement with the curves computed on basis of the statistical model in the approximation of three decay channels for the compound nucleus. Even at the energy of 5.92 MeV, where the excitation function of the integrated cross section displays a maximum, the statistical model predicts the shape of the angular distribution in a satis-

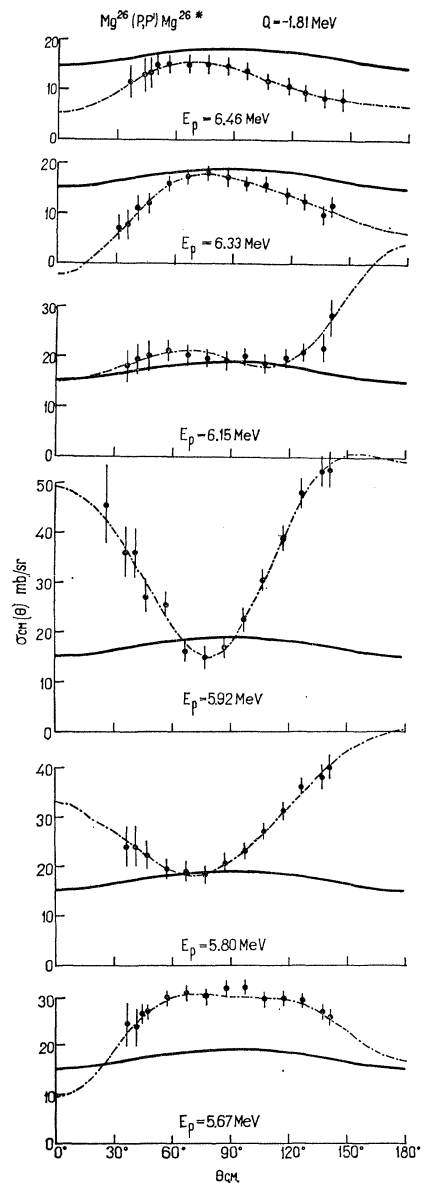


FIG. 7. The angular distributions of the protons inelastically scattered on the first Mg^{26} excitation level ($Q = -1.81$ MeV). The solid curves are computed on basis of the statistical model. The dashed curves are of the form (1), fitted by the least-squares method.

factory manner. The agreement with the statistical model reveals that in the case of the scattering on the second Mg²⁶ excited state, the interference effects are very small.

Angular Correlations. To obtain more extensive information on the reaction mechanism, angular-correlation measurements were also performed. The Mg²⁶ (*p*, *p'*γ), *Q* = -1.81 MeV angular correlations corresponding to the angles of 60°, 90°, and 120° of the proton detectors and taken at energies of 5.67, 5.80, 5.92, 6.15, and 6.46 MeV are shown in Figs. 9-13. Since measurements of the absolute double differential cross section were not made, the angular correlations are given in arbitrary units. Comparison with the predictions of different reaction theories is thus made only on the basis of the shape of the correlation curves. In view of the fact that the solid angle which the γ crystal subtends at the center of the target is comparatively small and that the experimental angular correlations do not display strong oscillations, the finite-solid-angle correction was not made. The solid curves computed on the basis of the statistical model were normalized to the experimental points. The dashed curves are of the form (2) and were drawn using the least-squares method. In Table II the quantities thus obtained are given. The

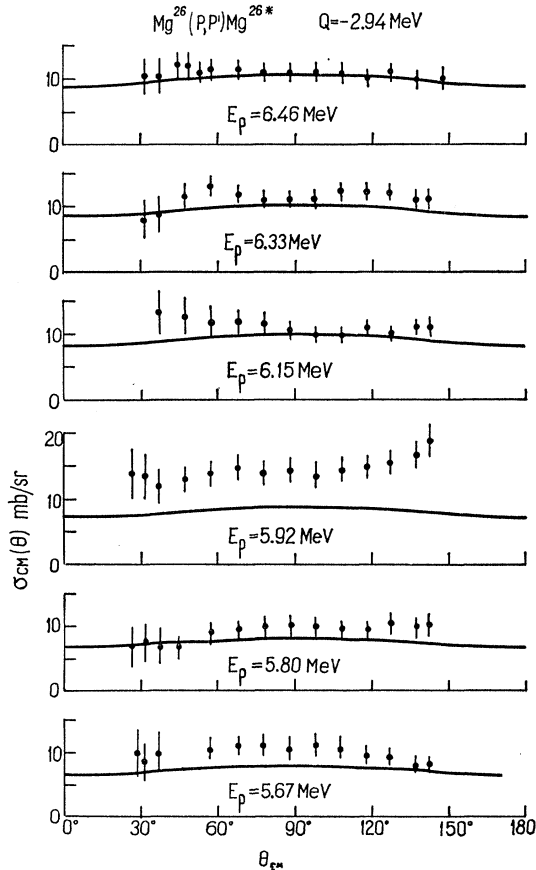


FIG. 8. The angular distributions of the protons inelasticly scattered on the second Mg²⁶ excitation level (*Q* = -2.94 MeV). The solid curves show the predictions of the statistical model.

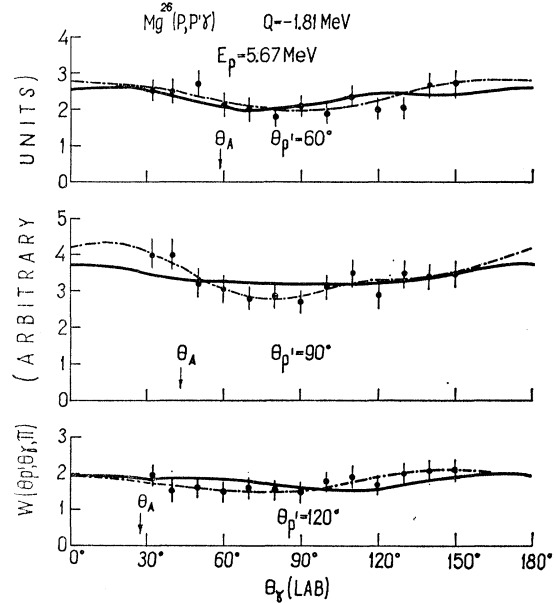


FIG. 9. The (*p*, *p'*γ) angular correlation between the protons inelasticly scattered on the first Mg²⁶ excited state (*Q* = -1.81 MeV) and the de-excitation gamma rays at *E_p* = 5.67 MeV. The solid curves are computed on the basis of the statistical model, while the dashed curves represent the least-squares fits of function (2) to the experimental data. θ_A is the adiabatic recoil angle.

shapes of the experimental angular-correlation curves undergo variations with the energy of the incident protons. At energies of 5.67, 5.80, and 5.92 MeV the experimental points, within the limits of the experimental errors, come sufficiently near to the curves computed with the help of the statistical model. Likewise, the values of the ratios *b/a* and *c/a* in Table II do not contradict, at these energies, the preponderance of the compound-nucleus mechanism. However, it is interesting to notice that at energies of 5.80 and 5.92 MeV the angular distributions show the greatest deviation from the statistical model. This suggests that the angular correlations are less sensitive to interference effects than the angular distributions, at least in this particular case. If this low sensitivity of the angular correlations to in-

TABLE II. Experimental values of the parameters of the angular correlations [Eq. (2)].

<i>E_p</i> (MeV)	θ _{<i>p</i>'} (deg)	<i>b/a</i>	<i>c/a</i>	θ ₀ (deg)	θ ₀ ' (deg)
5.67	60	0.06	0.43	2	95
	90	0.16	0.08	66	29
	120	0.08	0.37	87	65
5.80	60	0.69	0.76	59	107
	90	0.45	0.17	62	70
	120	0.44	0.49	88	80
5.92	60	0.23	0.37	82	67
	90	0.40	0.35	50	67
	120	0.27	0.75	26	68
6.15	60	0.87	0.07	60	91
	90	0.82	0.31	46	39
	120	0.13	0.84	30	63
6.46	60	1.71	0.62	51	108
	90	0.17	0.37	29	67
	120	1.72	1.14	44	87

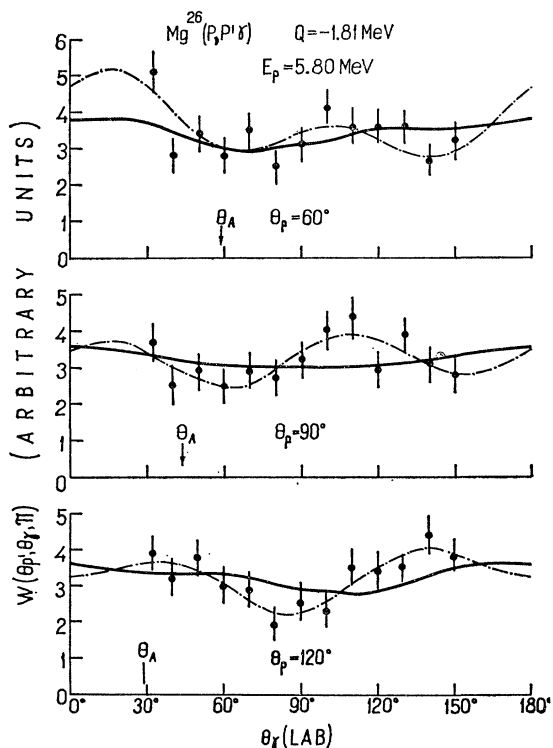


FIG. 10. As in Fig. 9 but for $E_p = 5.80$ MeV.

interference effects is also maintained at the energies of 6.15 and 6.46 MeV, then the higher oscillation amplitude of the angular correlations corresponding to these energies could be ascribed to some contributions of the

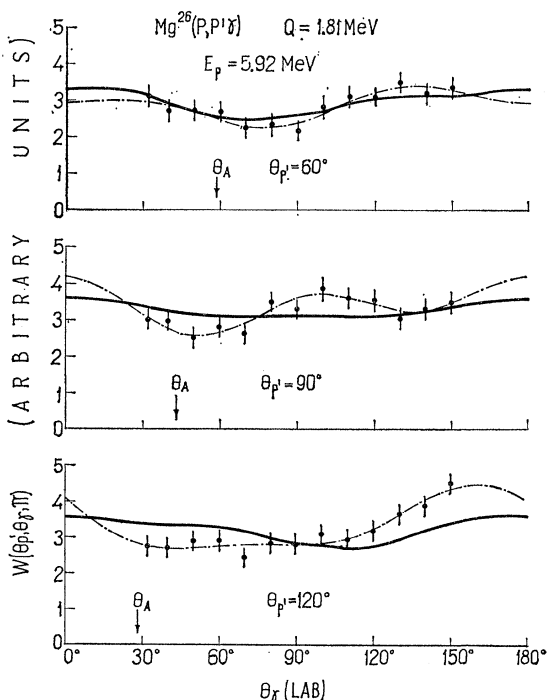


FIG. 11. As in Fig. 9 but for $E_p = 5.92$ MeV.

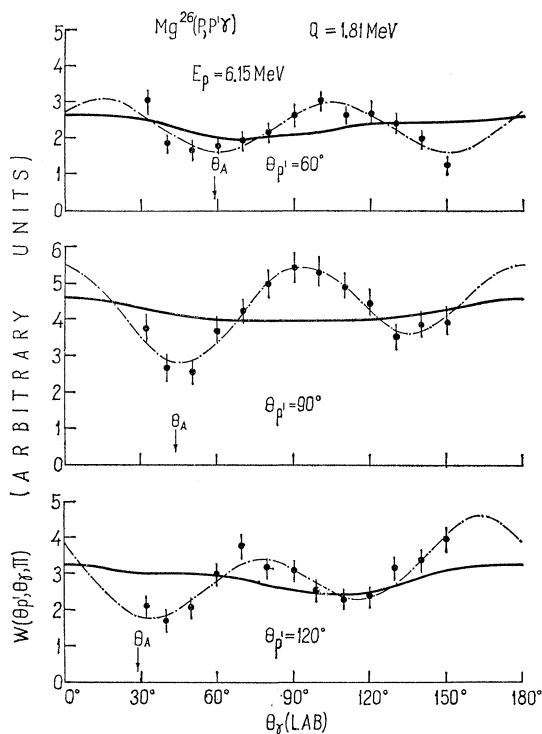


FIG. 12. As in Fig. 9 but for $E_p = 6.15$ MeV.

direct-interaction mechanism. Excepting the correlation corresponding to $\theta_{p'} = 90^\circ$ at the energy of 6.46 MeV, the angular correlations in Figs. 12 and 13 have the angle θ_0 near the adiabatic recoil angle $\theta_0 = \frac{1}{2}\pi - \frac{1}{2}\theta_{p'}$, in agreement with the predictions of the direct-interaction theory. However, this conclusion about the presence of

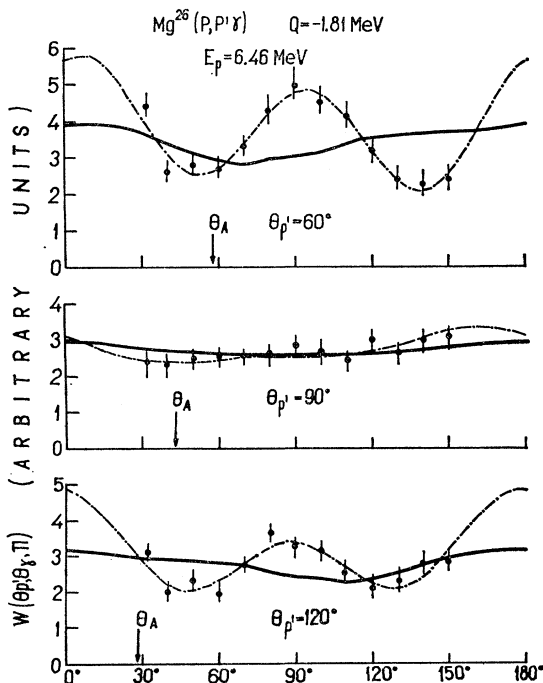


FIG. 13. As in Fig. 9 but for $E_p = 6.46$ MeV.

the D.I. mechanism at the energies of 6.15 and 6.46 MeV must be accepted with some limitations. Thus, as is seen in Table II, the ratio *b/a* exceeds unity only in the case of angular correlations corresponding to the angles $\theta_{p'} = 60^\circ$ and 120° at the energy of 6.46 MeV. Moreover, at both 6.15 and 6.46 MeV the angles θ_0 and θ_0' greatly differ from each other, in contradiction with the requirements of the direct-interaction theory. On the other hand, the intermixture of the two reaction mechanisms could justify these deviations.

The angular correlations between the protons inelastically scattered on the second Mg²⁶ excited state and the second γ radiation from the 2⁺ → 2⁺ → 0⁺ cascade were also measured, isotropic curves being obtained in all the cases. In Figs. 14 and 15 only the angular correlations corresponding to the energies 5.67 and 6.46 MeV are given, those obtained at the other energies being similar. The curves computed with the aid of the statistical model, using Sheldon's¹¹ formulas, are also shown. The solid curves were computed on the hypothesis that the 2⁺ → 2⁺ transition corresponding to the unobserved γ transition had been pure *M1*, and the dashed curves on the hypothesis of a pure quadrupole transition *E2*. Within the limits of experimental errors, both curves are in good agreement with the experimental data, the difference between them being too small to decide in favor of one or the other. However, a χ² test shows that the curve corresponding to a pure *M1* transition agrees somewhat better with the experimental data than the curve corresponding to the pure *E2* transition of the undetected γ radiation. This fact agrees with the meas-

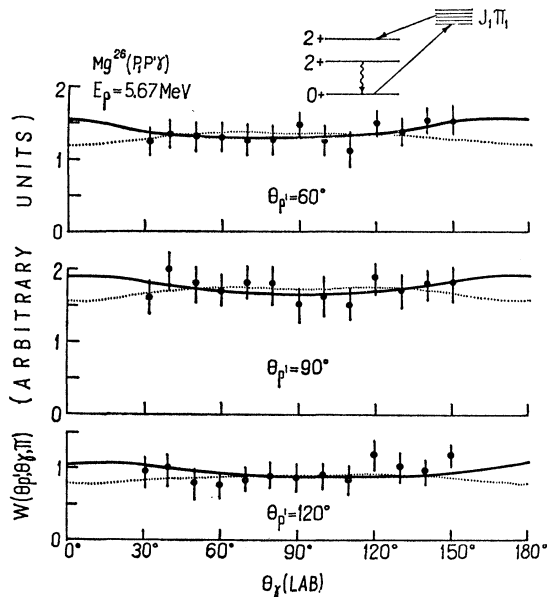


FIG. 14. The (*p, p'*γ) angular correlation between the protons inelastically scattered on the second Mg²⁶ excited state and the 1.81 MeV de-excitation gamma ray for the first level at $E_p = 5.67$ MeV. The solid curves were computed on basis of the statistical model, assuming for the unobserved gamma radiation a pure *M1* multipolarity, and the dashed curves were computed assuming a pure *E2* multipolarity.

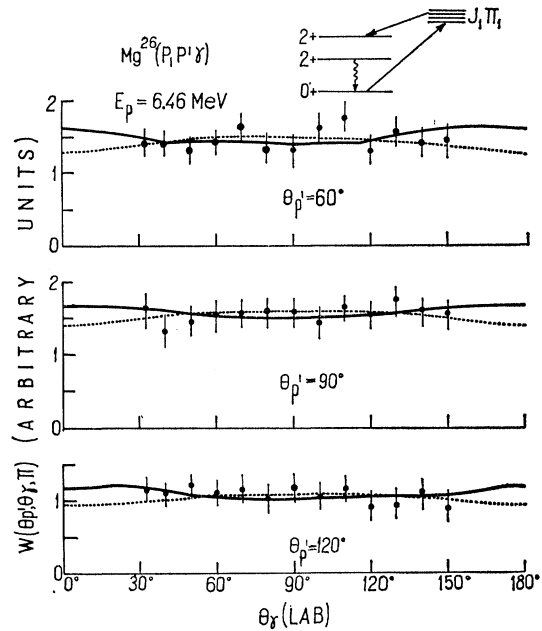


FIG. 15. As in Fig. 14 but for $E_p = 6.46$ MeV.

urements of Broude and Gove¹³ who obtained the value 0.12 for the *E2-M1* mixing ratio.

CONCLUSIONS

The experimental data presented in this paper show that at energies of the bombarding protons around 6 MeV, the predominant mechanism in the Mg²⁶(*p, p'*γ) reaction is that of the compound nucleus. The angular distributions and angular correlations corresponding to the excitation of the second Mg²⁶ level are well described by the statistical model for the nuclear reactions. Nevertheless, this model cannot account for the strong variation of angular distribution with energy, for the protons that leave Mg²⁶ in its first excited state. This fact implies that in the compound Al²⁷ nucleus, at excitation energies of about 14 MeV, the level density is high, but not sufficiently high for the interference between the partial proton waves to vanish. The comparison of the angular distributions corresponding to the excitation of the two Mg²⁶ levels with the predictions of the statistical model shows that the interference terms accounting for the deviations from this model are negligible in the case of scattering on the second excited state. The spin and parity of the residual nucleus being the same (2⁺) in both angular-distribution cases, the difference in their behavior can only be caused by the energy difference of the protons scattered on the two levels. But the angular distributions depend on energy through the transmission coefficients *T_l*(*E*). The transmission coefficients of the protons inelastically scattered on the second Mg²⁶ level have very small values for *l* > 1. This suggests that the interference terms are strongly related

¹³ C. Broude and H. E. Gove, Ann. Phys. (N. Y.) 23, 71 (1963).

to the partial waves with $l > 1$, thus manifesting themselves only in the angular distributions corresponding to the first excited state.

The form of the experimental angular correlations corresponding to the second excited state is well explained by the statistical model, confirming the conclusions drawn on the basis of the angular distributions about the preponderance of the compound-nucleus mechanism. The angular correlations corresponding to the first Mg^{26} excitation level come nearer to the predictions of the statistical model than did the angular distributions, suggesting that the interference effects are less prominent in the angular correlations. The greater deviations of the angular-correlation curves from the predictions of the statistical model at energies higher than 6 MeV could be caused by some contribution of the direct interaction. The probability for a D.I. contribution is also stronger, owing to the fact that at energies higher than 6 MeV the integrated inelastic cross section is smaller than that at energies lower than 6 MeV, which could correspond to a decrease of the C.N. weight.

The data in this work indicate that an important part in determining the shape of the angular distributions and angular correlations is played by the height of the excitation energy in the compound nucleus and by the value of the excitation energy of the residual nucleus level. The nearness to the predictions of the statistical model, found in many of the measured cases, is due to

the excitation of a comparatively large number of levels in the Al^{27} compound nucleus.

On the other hand, the good agreement of the angular distributions and correlations corresponding to the second Mg^{26} excitation level with the predictions of the statistical model is due to the higher value of the excitation energy of the residual nucleus level, which leads to the decrease in importance of the interference terms. This fact was also observed in the angular distributions of the protons scattered on the first two P^{31} excited states measured in this laboratory.¹⁴ While the angular distributions corresponding to the P^{31} first-excited state showed shape fluctuations at some energies, the angular distributions connected with the excitation of the second level kept their shape, in good agreement with the predictions of the statistical model.

In the case of the $Mg^{24}(p,p'\gamma)$ reaction theoretically analyzed by Sheldon,⁶ the experimental data did not agree with the statistical theory, thus confirming the importance of the compound-nucleus excitation energy, which is in this case about 6 MeV lower than in the case of the $Mg^{26}(p,p'\gamma)$ reaction.

ACKNOWLEDGMENTS

The authors thank the cyclotron staff and I. Huştea for technical assistance.

¹⁴H. Hulubei, M. Ivaşcu, A. Berinde, I. Neamu, N. Scîntei, I. Francz, N. Martalogu and E. Marincu, *Rev. Roumaine Phys.* (to be published).

Electron Scattering From Nuclear Magnetic Moments

T. A. GRIFFY*

High-Energy Physics Laboratory, Stanford University, Stanford, California

AND

D. U. L. YU†

Institute of Theoretical Physics, Department of Physics, Stanford University, Stanford, California

(Received 14 April 1965)

The elastic scattering of high-energy electrons from the magnetic dipole and magnetic octupole moments of light nuclei is calculated using shell-model wave functions. The results of the calculation are compared with recent experimental results for Be^9 and B^{11} and the possibility of obtaining a value for the magnetic octupole moment from an analysis of these experiments is discussed.

I. INTRODUCTION

IT is well known that elastic scattering of high-energy electrons is quite useful in investigating the charge distribution of nuclei.¹ More recently the experiments of Rand *et al.*² have shown that one may obtain con-

siderable information regarding the magnetic structure of nuclei by measuring the cross section for electron scattering at 180° . (One chooses a scattering angle of 180° since, from arguments based on time-reversal invariance and parity conservation, one can show that only odd magnetic-multipole moments contribute to the elastic-scattering cross section.³) This technique has been used previously to investigate inelastic scattering from various light nuclei⁴ and some investigation

* Supported in part by the U. S. Office of Naval Research through Contract No. Nonr-225(67).

† Supported by the U. S. Air Force through Air Force Office of Scientific Research Contract No. 49(638)-1389.

¹R. Hofstadter, *Ann. Rev. Nucl. Sci.* **7**, 231 (1957).

²R. E. Rand, R. Frosch, and M. R. Yearian, *Phys. Rev. Letters* **14**, 234 (1965).

³R. H. Pratt, J. D. Walecka and T. A. Griffy, *Nucl. Phys.* **64**, 677 (1965).

⁴W. C. Barber, *Ann. Rev. Nucl. Sci.* **12**, 1 (1962).